1996

Extended Kalman Filter for Photographic Data from Impact Acceleration Tests

Edit J. Kaminsky
University of New Orleans, ejbourge@uno.edu

R. E. Trahan
University of New Orleans

P. M. Chirlian
University of New Orleans

B. King
University of New Orleans

Recommended Citation

Kaminsky, E. J., R. E. Trahan, P.M. Chirlian, and B. King, "Extended Kalman Filter for Photographic Data from Impact Acceleration Tests," IASTED Signal and Image Process. Cont. Proc. (SIP'96), Orlando, FL, Nov. 11-14, 1996, pp. 59-63.

Proceedings of the IASTED International Conference
Signal and Image Processing (SIP '96)
November 11-14, 1996 Orlando, Florida USA

Extended Kalman Filter for Photographic Data from Impact Acceleration Tests

E. J. Kaminsky, R. E. Trahan, P. M Chirlian, and B. King
Department of Electrical Engineering
University of New Orleans
New Orleans, LA 70148
(504) 280-5616 (tel) (504) 280-3950 (fax)
ejbee@uno.edu

Abstract

This paper[1] presents the development of an Extended Kalman Filter (EKF) that optimally processes photographic data collected during short-duration impact acceleration tests. The system is modeled by a non-linear state-space representation using quaternions for rotational kinematics. Three cameras are used to photograph up to 14 fiducials mounted on a plate attached to the subject's mouth. The filter yields the history of the rotational and translational kinematics of the origin of the mouth plate. Results from the EKF and analysis of the estimation error are presented.

Keywords: *Extended Kalman filter, Impact acceleration, nonlinear systems, kinematics, photographic data, quaternions.*

Introduction

The Naval Biodynamics Laboratory (NBDL) conducts short-duration sled impact experiments [1] where a human subject or an anthropomorphic dummy sits on a sled which is suddenly given impetus to travel down a track. Data from three high speed photographic cameras mounted on the sled at about 1 meter from the subject are collected to determine the position of photographic targets mounted on various locations on the plate [2]. Linear acceleration data is also gathered with arrays of accelerometers placed on the subject's mouth and neck and on the sled.

NBDL processes photographic and accelerometer data independently to provide information about the kinematics of the system; the software is called EASYFLOW. A least squares algorithm is used by NBDL to determine the linear displacement and orientation parameters from photographic data [3], while integration techniques are used for the accelerometer data. Low frequency errors result in sharp discontinuities in the least squares photo solutions. Accelerometer-derived kinematic variables are best at the angular and linear acceleration and velocity levels, while photo-derived variables are best at the linear displacement and angular orientation levels.

NBDL researchers suggested in [4] that the results of these two measuring systems should be combined into one consistent and optimal set of kinematic variables from the acceleration to the displacement level. In response to this, researchers from NBDL and the University of New Orleans (UNO) are conducting work on combining the accelerometer and photographic data with an Extended Kalman Filter (EKF) to optimally determine the kinematics of the impact acceleration system. The system currently consists of two EKFs, one for accelerometer data, described in the companion paper [5], and another filter for photo data. This paper concentrates on the latter.

The System

The following state space formulation of the the impact acceleration test system is used:

$$\begin{aligned} x(t_{k+1}) &= \boldsymbol{f}\left(x(t_k), u(t_k), w(t_k), t_k\right) \\ y(t_k) &= \boldsymbol{h}\left(x(t_k), u(t_k), \zeta(t_k), t_k\right) \end{aligned} \qquad (1)$$

where $\boldsymbol{f}$ and $\boldsymbol{h}$ are the non-linear system and observable functions for the state vector x and the observable vector y; the sampling period is $t_{k+1} - t_k$, u is the input, and w and ς represent plant and measurement noise, respectively. Our system description is based on that presented in [6]. The state variables are the elements of the column state vector x, with x given by

$$x = [y_1, y_2, y_3, z_1, z_2, \cdots, z_9, q_1, q_2, \cdots, q_{12}]^T \qquad (2)$$

The first 12 states describe the translational kinematics of the system, the other 12 represent the rotational kinematics using quaternions. Table I lists the state variables. The input u is given by

[1]This research was funded by ONR Grant No. N00014-94-1-0990 and performed by UNO for the Naval Biodynamics Laboratory.

$$u=\left(0,0,\dot{a}_{xs},0,0,0,0,0,0,\dot{a}_{xa},0,\cdots,0\right) \qquad (3)$$

The discrete system assumes the acceleration increment over the nominal input u is modeled by a zero-mean white noise sequence, and is therefore a third order model. The state function, f, is obtained from the equations of motion with zero jerk, as given in Table II, where the bar over the quaternions indicate the variable before normalization.

Table I: State Variables

Variable	Description (Units)
y_1, y_2, y_3	x coordinate of the position, velocity, and acceleration of the sled w.r.t. lab, (m, m/s, m/s^2), respectively.
z_1, z_2, z_3	x, y, and z coordinates of translational position of the origin of the array frame[2] w.r.t sled (m).
z_4, z_5, z_6	x, y, and z coordinates of translational velocity of the origin of the array w.r.t sled (m/s).
z_7, z_8, z_9	x, y, and z coordinates of translational acceleration of the center of the array w.r.t. sled (m/s^2).
q_1, q_2, q_3, q_4	Quaternion rotational position of the array frame w.r.t. sled.
q_5, q_6, q_7, q_8	Quaternion rotational velocity of the array frame w.r.t. sled (s^{-1}).
$q_9, q_{10}, q_{11}, q_{12}$	Quaternion rotational acceleration of the array frame w.r.t. sled (s^{-2}).

Table II: State Variable Update

$y_1(t_{k+1}\|t_k)=y_1(t_k)+y_2(t_k)\left[t_{k+1}-t_k\right]+\frac{1}{2}y_3(t_k)\left[t_{k+1}-t_k\right]^2$
$y_2(t_{k+1}\|t_k)=y_2(t_k)+y_3(t_k)\left[t_{k+1}-t_k\right]$
$y_3(t_{k+1}\|t_k)=y_3(t_k)+u_{xs}(t_{k+1})-u_{xs}(t_k)$
$z_j(t_{k+1}\|t_k)=z_j(t_k)+z_{j+3}(t_k)\left[t_{k+1}-t_k\right]+\frac{1}{2}z_{j+6}(t_k)\left[t_{k+1}-t_k\right]^2$ $j=1,2,3$
$z_{j+3}(t_{k+1}\|t_k)=z_{j+3}(t_k)+z_{j+6}(t_k)\left[t_{k+1}-t_k\right],\quad j=1,2,3$
$z_7(t_{k+1}\|t_k)=z_7(t_k)+u_{xa}(t_{k+1})-u_{xa}(t_k)$
$z_{j+6}(t_{k+1}\|t_k)=z_{j+6}(t_k),\quad j=2,3$
$\overline{q_j}(t_{k+1}\|t_k)=q_j(t_k)+q_{j+4}(t_k)\left[t_{k+1}-t_k\right]+\frac{1}{2}q_{j+8}(t_k)\left[t_{k+1}-t_k\right]^2$ $j=1,\cdots,4$
$\overline{q_{j+4}}(t_{k+1}\|t_k)=q_{j+4}(t_k)+q_{j+8}(t_k)\left[t_{k+1}-t_k\right],\quad j=1,\cdots,4$
$\overline{q_{j+8}}(t_{k+1}\|t_k)=q_{j+8}(t_k),\quad j=1,\cdots,4$

The linearized discrete-time state variable system used to describe the impact test system is given in (4), where $\bar{x}$ is the linearized state vector, $\hat{A}$ is the linearized state transition matrix given in (5), and $\hat{C}$ is the observables Jacobian matrix of (6).

$$\begin{aligned}\bar{x}(t_{k+1})&=\hat{\boldsymbol{A}}\bar{x}(t_k)+\boldsymbol{B}u(t_k)+w(t_k)\\ \bar{y}(t_k)&=\hat{\boldsymbol{C}}(t_k)\bar{x}(t_k)+\boldsymbol{D}u(t_k)+\zeta(t_k)\end{aligned} \qquad (4)$$

$$\hat{\boldsymbol{A}}(t_k)=\left.\frac{\partial f(x,u,t)}{\partial x}\right|_{x=\hat{x}(t_k|t_k)} \qquad (5)$$

$$\hat{\boldsymbol{C}}(t_k)=\left.\frac{\partial \boldsymbol{h}(x,u,t)}{\partial x}\right|_{x=\hat{x}(t_k|t_{k-1})} \qquad (6)$$

[2]The origin of the accelerometer array frame is the origin of the instrumentation CS.

The "raw photo data" collected are two coordinates of filmplane measurements. The observable vector y, obtained from triangulation on the raw data, can be written as

$$y=[f_{11},f_{12},f_{13},f_{21},\cdots,f_{N3}] \qquad (7)$$

where N is the number of photo targets on the mount, and the first index indicates the coordinates x, y, and z of each fiducial f_i. The non-linear function h is given, in quaternion notation, by

$$f_i=\left(0,f_{i1},f_{i2},f_{i3}\right)=(0,z_1,z_2,z_3)+qe_iq^* \qquad (8)$$

with e_i is the quaternion position of photo-target i, and z and q are the components of interest of the state vector (position and rotation). Stereovideography is used to determine the position of each fiducial in the mount; this process yields the vectors e_i of (8). We add three ideal observations (δ_1, δ_2, δ_3) to the observables in the vector y to account for the quaternion normalization.

The equations for the EKF are:

$$\begin{aligned}
P(t_k|t_{k-1}) &= \hat{A}P(t_{k-1}|t_{k-1})\hat{A}^T+Q(t_k)\\
G(t_k) &= P(t_k|t_{k-1})\hat{C}(t_k)^T\\
&\quad\times\left[\hat{C}(t_k)P(t_k|t_{k-1})\hat{C}(t_k)^T+R(t_k)\right]^{-1}\\
\hat{x}(t_k|t_k) &= \hat{x}(t_k|t_{k-1})+G(t_k)\\
&\quad\times\left[y(t_k)-h(\hat{x}(t_k|t_{k-1}))\right]\\
\hat{x}(t_{k+1}|t_k) &= \hat{A}\hat{x}(t_k)+\hat{B}u(t_k)\\
P(t_k|t_k) &= P(t_k|t_{k-1})-G(t_k)\hat{C}(t_k)P(t_k|t_{k-1})
\end{aligned} \qquad (9)$$

where Q is the plant noise covariance, R is the measurement noise covariance, $P(t_k|t_{k-1})$ is the covariance of the estimation error and $G(t_k)$ is the filter gain.

Quaternion Constraints

Due to the nature of quaternions and their use in representing rotation matrices, certain constraints must be met by the state variables representing them. These constraints are given in Table III, and state that quaternions have a unity norm, and that the first and second derivatives of the quaternion norm are equal to zero. These are the constraints used for normalization of the quaternions after the state update.

Table III: Quaternion Constraints

$$\delta_1\doteq\|q\|-1=\sum_{i=1}^{4}q_i^2-1$$

$$\delta_2=\dot{\delta}_1=\frac{d}{dt}\|q\|=\sum_{i=1}^{4}q_iq_{i+4}$$

$$\delta_3=\ddot{\delta}_1=\frac{d^2}{dt^2}\|q\|=\sum_{i=1}^{4}q_iq_{i+8}+\sum_{i=1}^{4}q_{i+4}^2$$

The Initial Conditions

Initial conditions for each of the 24 states are needed in order to filter the raw data. It is desirable to have a good estimate of the initial conditions of the system in order to produce good estimates. The ideal system is initially at rest (i.e. all velocities and accelerations are zero), but the actual subject is moving slightly. The initial conditions needed to initialize the EKF are currently derived from EZFLOW processed data provided by NBDL. We average pre-impact samples for the state estimates provided to obtain the mean starting position, velocity, and acceleration of the sled and mouth mount, and the mean initial rotational position of the instrument coordinate system; other initial kinematics are set to zero. Using bars over the state variables to indicate averaging over 25 points, the initial state vector used by the EKF becomes:

$$\begin{aligned}
x=\big[&\bar{y}_1,0,0,\bar{z}_1,\bar{z}_2,\bar{z}_3,0,0,0,0,0,0,\\
&\bar{q}_1,\bar{q}_2,\bar{q}_3,\bar{q}_4,0,0,0,0,0,0,0,0\big]
\end{aligned} \qquad (10)$$

The Noise in the System

There are two noise sequences in the model: the plant noise, which includes uncertainties and inaccuracies in the model itself, and the measurement noise, which includes uncertainties, instrumentation errors, and measurement errors. The accuracy of the noise characterization greatly affects the performance of the Kalman filter and its convergence.

The plant noise is represented in eq. (4) by the term $w(t_k)$. In our model w is assumed to be an additive white gaussian noise (AWGN) signal with zero mean, and variance $\sigma_x^2(t_k)$, where the subscript x denotes we are dealing with the states. The default variance of most states is currently determined by the deviation of the EASYFLOW-processed data from the average over the ensemble of runs. A small variance is assumed for states not available from EASYFLOW. This yields the time-varying covariance matrix $Q(t_k)$.

The measurement noise, or noise in the observables, is represented in eq. (4) by the term $\zeta(k)$. We again make the assumption of zero-mean AWGN for the noise in the observations and assume all noise to be uncorrelated. Many sources of error (noise) that arise when making measurements using NBDL's photographic system and related calibration

equipment have been identified. The most significant are vibration, blur circle, error in sproket hole prediction, error in nodal point location, and digitization errors.

The standard deviation of the total photographic measurement noise, σ_y, is computed as the square root of the sum of the squares of the standard deviations of all noise components identified and quantified. The value for the standard deviation during preliminary tests of the photographic EKF was $\sigma_y = 2$ cm which, under the AWGN assumption, indicates that the measured (observed) location of the targets with respect to the sled coordinate system is within 2 cm of the true value 68% of the time and almost certainly within 6 cm. In future tests, the angular errors will be included as well, which then yields a standard deviation of $\sigma_y = 3.32$ cm.

Validation of the EKF using Photographic Data.

The EKF expects the observables to be the 3D coordinates of each fiducial with respect to the sled CS, f_i, while the relevant output is the position of the instrumentation origin with respect to the sled, (z_1, z_2, z_3). Since the triangulation algorithm that converts the 2D filmplane measurements to the 3D positions has not been implemented yet, we devised the following test of the EKF.

The states generated by EZFLOW are used to generate theoretical fiducial observables f_i; i.e., we "work backwards" from NBDL's processed data to obtain observables. These generated "observables" are then processed with the photo EKF as if they were actual measurements to generate the EKF states. The EKF states are then compared to the original EZFLOW states. Since this amounts, basically, to processing the observables twice, it is expected that the results of this test will yield states that are very similar to those produced by EZFLOW, but smoother. We believe that this method provides a valid test of the EKF model itself and of the code that implements the filter.

The EZFLOW photo data used during these tests are the position of the head (z_1, z_2, z_3) and the position quaternion (q_1, q_2, q_3, q_4), along with the location of the phototargets within the mouth array (e_i).

EKF Test Results

The tests of the photo EKF have produced encouraging results, with filter output that resembles the EZFLOW results and with an error covariance well within acceptable limits. The EKF produces good results for all kinematics, not just for position as is the case for EZFLOW; velocity and acceleration from the EKF are also reliable.

Figures 1 through 4 show results for run LX3858, comparing EZFLOW and EKF processed data when possible. Fig. 1 is a plot of the displacement of the origin of the inst CS with respect to the sled in the x direction versus time, z_1; both EZFLOW and EKF results are shown, and although the two curves do not overlap at all times, the results confirm the filter is performing well. As expected, the largest difference between data processed with EZFLOW and the EKF occurs at points where the kinematics change rapidly (at and right after impact). This is where the variance of the plant noise is largest.

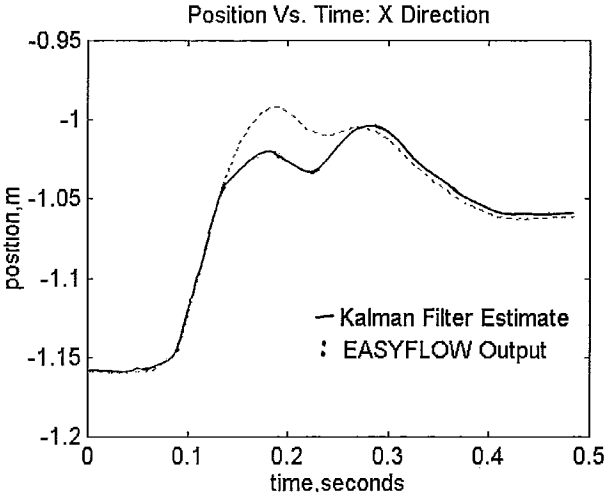

Figure 1: Z1 vs. time for run LX3858

The velocity curves for run LX3858 are shown in Fig. 2, where it is clear that the EKF filtered data nicely tracks the velocity of the head. The EKF produces velocity estimates that are much smoother than those generated by EZFLOW indicating that the former are a filtered version of the latter. We expect the velocity computed by the EKF to be smoother that that from EZFLOW even when the true observables are used. The state representing the acceleration of the mouth in the x direction versus time is shown in Fig. 3; photo-EZFLOW does not produce acceleration data so only the EKF curve is shown. Although we have chosen to show only the x-direction states, we must mention that all kinematics in all directions are provided by the EKF, with seemingly good results. The acceleration in the y direction is slightly noisier than the acceleration in the x direction.

A clear advantage of the EKF over other estimation methods is that it provides, through the error covariance matrix, an indication of how well the filter is performing, and whether the results are reliable. Fig. 4 shows the time history of the error covariance of the position in the x direction (z_1) for run LX3858. The error variance is no larger than 0.000265 m^2, i.e. a maximum standard deviation of 1.63 cm which amounts to about 9.5% of the total displacement in the x direction. This tells us that, assuming a Gaussian distribution, the estimate of the position in the x direction is within 1.628 cm of the true position 68% of the time, at the worst. Notice that the maximum deviation of about 1.63 cm in our estimate is smaller than the assumed deviation of 2 cm of the original data. Moreover, we can see that the results do not tend to grow as time passes; instead, the error covariance increases

after impact and then decreases again indicating that the filter does not diverge at any time.

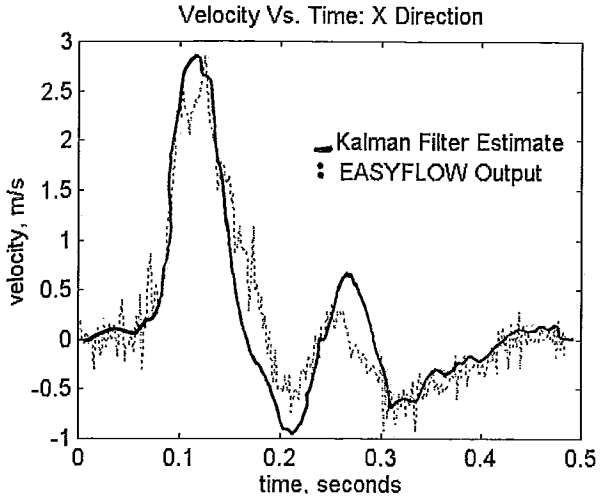

Figure 2: Z_4 vs. time for run LX3858

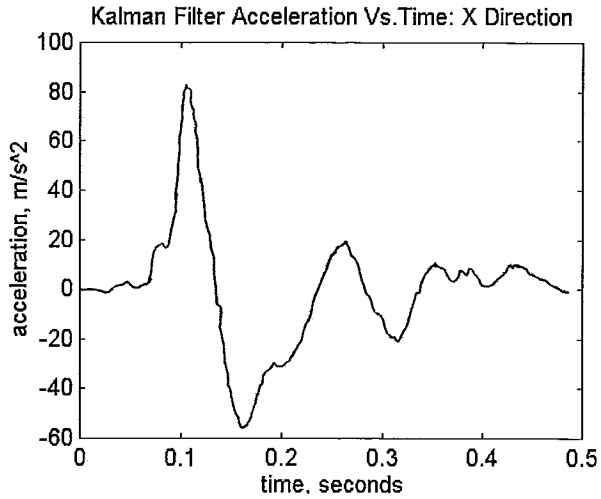

Figure 3: Z_7 vs. time for run LX3858

Further Work

A triangulation algorithm must be implemented to convert the 2D filmplane coordinates into the 3D spatial coordinates needed by the EKF. The photo EKF described here must be integrated with the EKF presented in [5] to optimally process accelerometer and photographic data simultaneously. Finally, the problem of missing phototarget data, where some targets appear or disappear from the cameras' view, must be solved.

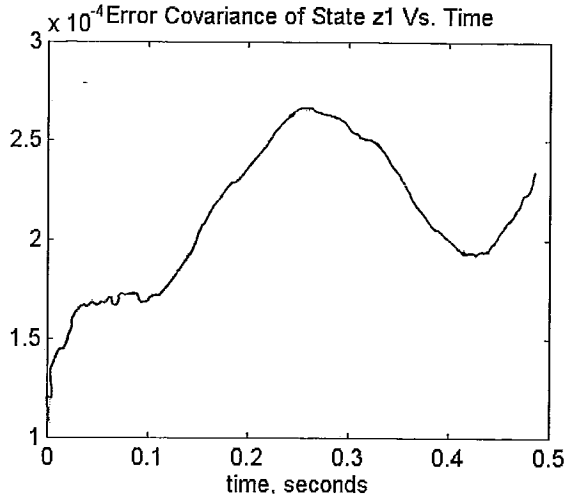

Figure 4: Error estimate for z_1 vs. time for run LX3858

References

[1] Willems, G., W. Muzzy, W. Anderson, and E. Becker, "Cinematography data systems at the Naval Biodynamics Laboratory," *SPIE Second Internat. Symposium of Biomechanics Cinematography and High Speed Photography*, vol. 291, pp.90-96, 1981.

[2] Becker, Edward, "A Photographic Data System for Determination of 3 Dimensional Effect of Multiaxes Impact Acceleration on Living Humans," *in Proc. SPIE Effective Utilization of Photographic and Optical Technology to the Problems of Automotive Safety, Emissions, and Fuel Economy,* vol 57, pp. 69-78, 1975.

[3] William H. Muzzy, III, A. M. Prell, and P. B. Shimp, "Camera and Site Calibration for Three-dimensional (3-d) Target Acquisition," *SPIE Second Internat. Symposium Biomechanics Cinematography and High-speed Cinematography*, , vol. 291, pp. 161-169, 1981.

[4] Lustick, L. S., H. G. Williamson, M. R. Seemann, and J. M. Bartholomew, "Problems of Measurement in Human Analog Research," *NBDL Research Report No. NBDL-82R012*, May 1982.

[5] Kaminsky, E. J., R. E. Trahan, P. M. Chirlian, and D. Malley, "Extended Kalman Filter for Accelerometer Data from Impact Acceleration Tests," *IASTED SIP'96 Signal and Image Proc. Conf. Proc.*, Orlando, FL, Nov. 11-14, 1996, paper no. 251-033.

[6] Ash, Michael E., "Simultaneous Processing of Photographic and Accelerometer Array Data from Sled Impact Experiments," The Charles Stark Draper Laboratory, Inc., (Cambridge, MA). Report number AFAMRL-TR-82-73, December, 1982.